Journal of Alloys and Compounds 509 (2011) 2493–2495

Contents lists available at ScienceDirect

Journal of Alloys and Compounds

journal homepage: www.elsevier.com/locate/jallcom

The electronic states calculated using the sinusoidal potential for $Cd_{1-x}Zn_xS$ quantum dot superlattices

A. Sakly[a], N. Safta[a,*], H. Mejri[b,c], A. Ben Lamine[a]

[a] Unité de Physique Quantique, Faculté des Sciences, Avenue de l'Environnement, 5000 Monastir, Tunisia
[b] Laboratoire d'Electronique et de Microélectronique, Faculté des Sciences, Avenue de l'environnement, 5000 Monastir, Tunisia
[c] Unité de Recherche de Mathématiques Appliquées et Physique Mathématiques, Ecole Préparatoire aux Académies Militaires, Avenue Maréchal Tito, 4029 Sousse, Tunisia

ARTICLE INFO

Article history:
Received 14 July 2010
Received in revised form 5 November 2010
Accepted 10 November 2010
Available online 18 November 2010

Keywords:
$Cd_{1-x}Zn_xS$
Flattened cylindrical quantum dots
Superlattice
Sinusoidal potential
Minibands

ABSTRACT

The present work reports on a theoretical investigation of superlattices based on $Cd_{1-x}Zn_xS$ quantum dots embedded in an insulating material. The system to model is assumed to be a series of flattened cylindrical quantum dots with a finite barrier at the boundary and is studied using a sinusoidal potential. The electronic states of both Γ_1 – (ground) and Γ_2 – (first excited) minibands have been computed as a function of inter-quantum dot separation and Zn composition. An analysis of the results shows that the widths of Γ_1 – and Γ_2 – minibands decrease as the superlattice period and Zn content increase separately. Moreover, the sinusoidal shape of the confining potential accounts for the coupling between quantum dots quantitatively less than the Kronig–Penney potential model.

© 2010 Elsevier B.V. All rights reserved.

1. Introduction

Until now, the study of $Cd_{1-x}Zn_xS$ thin films remains one of the primary interests in fundamental and applied researches as well [1–12]. In fact, $Cd_{1-x}Zn_xS$ is the most appropriate to be used as window layer material in solar cells based on conventional p-type absorber layer like $CuInSe_2$ [13,14] or on quaternary compounds such as $CuIn_xGa_{1-x}Se_2$ or $CuSnS_zSe_{1-z}$ [15].

To the subject of $Cd_{1-x}Zn_xS$ quantum dots (QDs), the potentiality of these nanostructures does not cease to be proved in many device applications [16–23,13,14,24]. In epitaxy, there has also been a progress in the growth of $Cd_{1-x}Zn_xS$ QDs [24–34]. Experimentally, a deal of interest is focused on the study of $Cd_{1-x}Zn_xS$ QDs using different characterization techniques [24,35,36]. More rigorously, $Cd_{1-x}Zn_xS$ QDs embedded in a dielectric matrix should be described theoretically by using a spherical model. Based on this geometry, two approaches have been adopted to model the confinement potential, a potential with an infinite barrier [24,32,37,38] and a potential with a finite barrier [39,40] at the boundary. The latter potential has the advantage to predict the electronic properties resulting from the coupling between QDs. However, the spherical geometry does not lend simply to calculate the band edges of coupled QDs, especially along different quantization directions.

In the present work, we attempt to study the coupling in the case of a chain based on $Cd_{1-x}Zn_xS$ QDs for which the confinement potential can be modelled using flattened cylindrical geometry, as reported in Ref. [41].

2. Theoretical formulation and results

In Fig. 1a, we report a schematic diagram of the chain mentioned above. Along a common direction, denoted by z, of spherical $Cd_{1-x}Zn_xS$ QDs, electrons and holes see a succession of flattened cylinders of radius R and an effective height L. The inter-quantum dot separation is labelled d, which corresponds to the period of structure. According to that reported in Ref [24], the diameter $D = 2R$ varies from 9 nm to 4 nm going from CdS to ZnS. Then, if we consider $L = 1$ nm which corresponds to the value reported in Ref. [42], it clearly appears that L is lower than D and thus the quantum confinement along transversal directions can be disregarded. As a consequence, the $Cd_{1-x}Zn_xS$ multi-quantum dot system can be considered as a superlattice (SL) along the longitudinal confined direction.

According to this scheme, the system to investigate is a $Cd_{1-x}Zn_xS$ QD superlattice where $Cd_{1-x}Zn_xS$ flattened cylinders correspond to quantum wells whereas the host dielectric lattice behaves as a barrier. For sake of simplicity, the electron and hole states are assumed to be uncorrelated. Thus, the problem to solve is reduced to those of one dimensional potential. In our previous work [41], we have adopted the Kronig–Penney model to describe

* Corresponding author.
E-mail address: saftanabil@yahoo.fr (N. Safta).

0925-8388/$ – see front matter © 2010 Elsevier B.V. All rights reserved.
doi:10.1016/j.jallcom.2010.11.059

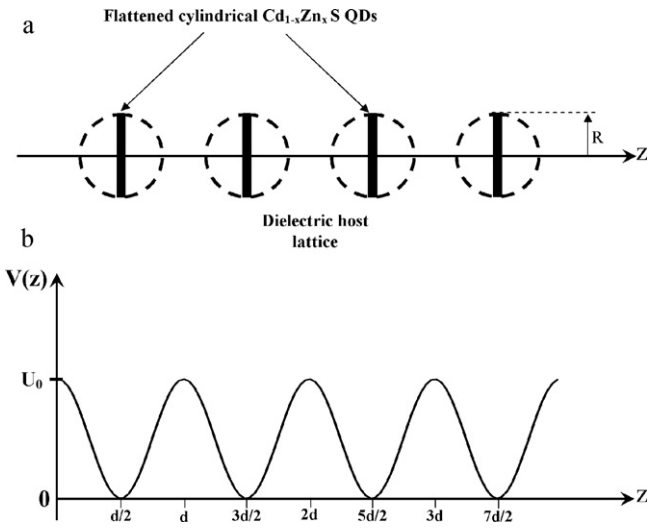

Fig. 1. (a) A schematic diagram of $Cd_{1-x}Zn_xS$ QD superlattices according to the flattened cylindrical geometry. (b) The sinusoidal potential used to calculate the subband structure.

the confinement potential. Such a potential is characterized by abrupt barriers. Using this model, we have calculated the ground and the first excited minibands for both electrons and holes. Calculations were made as a function of ZnS molar fraction and the inter-quantum dot separation. Using this model, we have also computed the longitudinal effective mass versus x and d as well. Really, the barriers separating QD wells are not abrupt and exhibit a progressive variation along the quantization direction z. In other hand, the confinement potential is periodic and thus can be developed on Fourier series as a function of z. The potential, being limited to the fundamental harmonic, can be expressed as:

$$V_{e,h}(z) = \frac{U_{0e,h}}{2}\left(\cos\frac{2\pi z}{d} + 1\right) \quad (1)$$

Here $U_{0e,h}$ is the barrier height between adjacent QDs. Fig. 1b shows the shape of this potential energy. Accordingly, the electron and hole states of QDs can be calculated from the Hamiltonien:

$$H_{e,h} = -\frac{\hbar^2}{2m^*_{e,h}}\frac{d^2}{dz^2_{e,h}} + \frac{U_{0e,h}}{2}\left(\cos\frac{2\pi z}{d} + 1\right) \quad (2)$$

where $\hbar$ is the Plank's constant, m^* is the effective mass of carriers. The subscripts e and h refer to electron and hole particles respectively. In deriving the Hamiltonien $H_{e,h}$, we have adopted the effective mass theory (EMT) and the band parabolicity approximation (BPA). The mismatch of the effective mass between the well and the barrier has been neglected. Values of the electron and hole effective masses for CdS and ZnS are taken from Ref. [42]. For $Cd_{1-x}Zn_xS$, these two parameters have been calculated using the linear interpolation. The barrier height $U_{0e,h}$ and the inter-sheet separation d are treated as parameters. Values of these parameters are taken from Refs [41,42]. Table 1 reports parameters used to calculate the Γ_1 – and Γ_2 – minibands for $Cd_{1-x}Zn_xS$ QD superlattices.

Table 1
Electron band parameters used to calculate the Γ_1 – and Γ_2 – minibands for $Cd_{1-x}Zn_xS$ QD superlattices.

x	$\frac{m^*_e}{m_0}$	U_{0e}(eV)
0.0	0.16	0.10
0.2		0.25
0.4		0.45
0.6		0.75
0.8		1.50
1.0	0.28	2.00

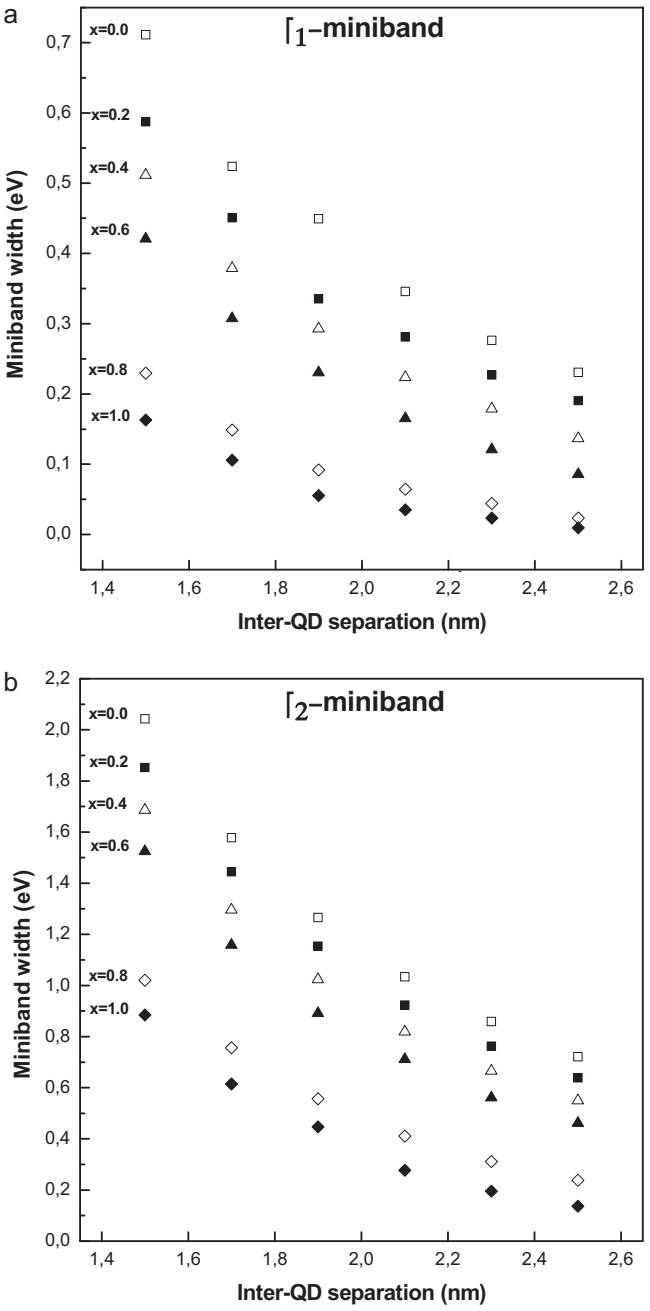

Fig. 2. The Γ_1 – (a) and Γ_2 – (b) miniband widths as calculated for electrons versus the inter-QD separation for different *Zn* compositions.

By solving the schrodinger equation corresponding to the Hamiltonien $H_{e,h}$, we have calculated the electron states of both Γ_1 – and Γ_2 – minibands for $Cd_{1-x}Zn_xS$ QD structures. Calculations were made versus Zn composition going from CdS to ZnS for different inter-QD separations. As has been found, for this model of potential, the major effect of decreasing this separation is to broaden the discrete states of isolated QDs into minibands. The latter trend is specific for SL structures. Typical results for the Γ_1 – miniband are depicted in Fig. 2a. Two peculiar features were revealed: (i) for any composition x, the width $\Delta E_{1,e}$ of the Γ_1 – miniband decreases with the increase of the SL period d (ii) the Γ_1 – miniband width shows a decreasing tendency with increased ZnS molar fraction independently to the inter-QD separation. It is worth noticing, from obtained results, that the difference between the Γ_1 – miniband widths for CdS QDs is equal to 0.481 eV whereas that of

Table 2
Widths of the Γ_1 – miniband for the present work (a) and those obtained by the Kronig–Penney potential (b) as reported in Ref. [41].

d (nm) / x	1.5	1.7	1.9	2.1	2.3	2.5
0	0.711[a]	0.523[a]	0.449[a]	0.345[a]	0.276[a]	0.230[a]
	0.727[b]	0.586[b]	0.468[b]	0.370[b]	0.312[b]	0.267[b]
0.2	0.587[a]	0.450[a]	0.335[a]	0.281[a]	0.226[a]	0.190[a]
	0.676[b]	0.533[b]	0.408[b]	0.306[b]	0.250[b]	0.216[b]
0.4	0.511[a]	0.379[a]	0.292[a]	0.223[a]	0.178[a]	0.136[a]
	0.586[b]	0.442[b]	0.306[b]	0.234[b]	0.175[b]	0.153[b]
0.6	0.420[a]	0.307[a]	0.230[a]	0.165[a]	0.120[a]	0.085[a]
	0.494[b]	0.325[b]	0.242[b]	0.153[b]	0.112[b]	0.075[b]
0.8	0.229[a]	0.148[a]	0.091[a]	0.064[a]	0.044[a]	0.023[a]
	0.331[b]	0.191[b]	0.102[b]	0.065[b]	0.037[b]	0.025[b]
1.0	0.162[a]	0.105[a]	0.055[a]	0.034[a]	0.023[a]	0.009[a]
	0.234[b]	0.130[b]	0.051[b]	0.039[b]	0.012[b]	0.012[b]

ZnS-related QDs is of 0.153 eV. For intermediate compositions, this difference is ranged between the two extreme values. For the QDs based on CdS, the coupling between nanoparticles shows a drastic drop as the inter-quantum dot separation increases. This trend is due mainly to the low potential barrier heights. Thus, the high coupling is governed by the tunnelling effect for shorter SL periods. By contrast, for larger inter QD separations, the tunnelling effect becomes relatively weak even if the barrier heights are low. On the other hand, for larger ZnS molar fractions, the coupling is less sensitive to the decreasing of d. This behaviour can be explained in terms of the largeness of barrier height. For the width of the first excited miniband $\Delta E_{2,e}$ the same variation versus the SL period d has been achieved as depicted in Fig. 2b. Except that the effect of d on the delocalization of electrons in Γ_2 – miniband is more noticeable. For comparison with results obtained by using the Kronig–Penney model [41], we report in Table 2 widths of Γ_1 – miniband as calculated in the present work and those reported in Ref. [41]. As can be noticed, practically for all the Zn compositions and inter sheet QD separations studied, the Γ_1 – miniband widths of this work are slightly lower. Interestingly, the sinusoidal potential does not account for the coupling as much as than the Kronig–Penney potential model. The reason is the progressive barrier which characterizes the change of the sinusoidal potential.

3. Conclusions

We have investigated the superlattice behaviour in multi-quantum dot structures based on $Cd_{1-x}Zn_xS$. The QDs are described using a flattened cylindrical geometry with a finite potential barrier at the boundary. To simulate the confining potential, we have adopted the sinusoidal shape. Based on this potential model, we have calculated the ground and the first excited minibands for electrons. Calculations have been made as a function of the inter-QD separation and Zn composition. An analysis of the results has evidenced that: (i) the widths of Γ_1 – and Γ_2 – minibands are found to be decreasing with d and x separately (ii) for all the Zn compositions and inter-sheet QD separations studied, the miniband widths of the present work are slightly lower compared to that obtained by the Kronig–Penney potential.

References

[1] Z. Zhou, K. Zhao, F. Huang, Mater. Res. Bull. 45 (2010) 1537–1540.
[2] L. Wang, W. Wang, M. Shang, W. Yin, S. Sun, L. Zhang, Int. J. Hydrogen Energy 35 (2010) 19–25.
[3] M. Mnari, N. Kamoun, J. Bonnet, M. Dachraoui, C. Rend. Chimie 12 (2009) 824–827.
[4] T. Özer, S. Köse, Int. J. Hydrogen Energy 34 (2009) 5186–5190.
[5] M. Li, J. Jiang, L. Guo, Int. J. Hydrogen Energy 35 (2010) 7036–7042.
[6] F. del Valle, A. Ishikawa, K. Domen, J.A. Villoria de la Mano, M.C. Sánchez-Sánchez, I.D. González, S. Herreras, N. Mota, M.E. Rivas, M.C. Álvarez Galván, J.L.G. Fierro, R.M. Navarro, Catal. Today 143 (2009) 51–56.
[7] W. Xia, J.A. Welt, H. Lin, H.N. Wu, M.H. Ho, C.W. Tang, Sol. Energy Mater. Sol. Cells 94 (2010) 2113–2118.
[8] Y. Raviprakash, K.V. Bangera, G.K. Shivakumar, Sol. Energy 83 (2009) 1645–1651.
[9] Y. Raviprakash, Kasturi V. Bangera, G.K. Shivakumar, Curr. Appl. Phys. 10 (2010) 193–198.
[10] N.A. Noor, N. Ikram, S. Ali, S. Nazir, S.M. Alay-e-Abbas, A. Shaukat, J. Alloys Compd. 507 (2010) 356–363.
[11] Z. Nourbakhsh, J. Alloys Compd. 505 (2010) 698–711.
[12] P.P. Hankare, P.A. Chate, D.J. Sathe, J. Alloys Compd. 487 (2009) 367–369.
[13] H.H. Gürel, Ö. Akinci, H. Ünlü, Thin Solid Films 516 (2008) 7098–7104.
[14] M. Gunasekaram, M. Ichimura, Sol. Energy Mater. Sol. Cells 91 (2007) 774–778.
[15] N. Gawedang, T. Gawedang, Mater. Lett. 59 (2005) 3577.
[16] V. Alberts, R. Herberhonz, T. Walter, H.W. Scock, J. Phys. D: Appl. Phys. 30 (1997) 2156.
[17] N. Kohara, T. Negami, M. Nishitani, T. Wada, Jpn. J. Appl. Phys. 34 (1995), L1141.
[18] H.L. Kwok, J. Phys. D: Appl. Phys. 16 (1983) 2367.
[19] H.S. Kim, H.B. Im, J.T. Moon, Thin Solid Films 214 (1992) 207–212.
[20] G. Gordillo, Sol. Energy Mater. Sol. Cells 25 (1992) 41.
[21] J.W. Bowron, S.D. Damaskinos, A.E. Dixon, Sol. Cells 31 (1991) 159.
[22] O.M. Hussain, P.S. Reddy, B.S. Naidu, U. Uthanna, P.J. Reddy, Semicond. Sci. Technol. 6 (1991) 690.
[23] T.L. Chu, S.S. Chu, J. Britt, C. Feredikes, C.Q. Wu, J. Appl. Phys. 70 (1991) 2688.
[24] B. Bhattacharjee, S.K. Mandal, K. Chakrabarti, D. Ganguli, S. Chaudhui, J. Phys. D: Appl. Phys. 35 (2002) 2636–2642.
[25] L. Cao, S. Huang, S. E, J. Colloid Interface Sci. 273 (2004) 478–482.
[26] H. Kumano, A. Ueta, I. Suemune, Phys. E 13 (2002) 441–445.
[27] Y. Cai Zhang, W. Wei Chen, X. Ya Hu, Mater. Lett. 61 (2007) 4847–4850.
[28] K. Tomihira, D. Kim, M. Nakayama, J. Lumin. 112 (2005) 131–135.
[29] J. Zhu, J. Zhang, J. Zhen, C. Chen, J. Lu, S. Chen, Physica B 405 (2010) 3452–3457.
[30] L. Song, H. Wei, H. Xu, J. Zhan, Mater. Res. Bull. 45 (2010) 1396–1400.
[31] S. Karamjit, N.K. Verma, H.S. Bhatti, Physica B 404 (2009) 300–304.
[32] K.K. Nanda, S.N. Sarangi, S. Mohanty, S.N. Sahu, Thin Solid Films 322 (1998) 21–27.
[33] P.B. Bagdare, S.B. Patil, A.K. Singh, J. Alloys Compd. 506 (2010) 120–124.
[34] L. Wang, M. Niu, Z. Wu, Curr. Appl. Phys. 9 (2009) 1112–1116.
[35] Y. Li, R. Yi, X. Liu, J. Alloys Compd. 486 (2009) L1–L4.
[36] Q. Wang, G. Chen, C. Zhoua, R. Jin, L. Wang, J. Alloys Compd. 503 (2010) 485–489.
[37] H. Yükselici, P.D. Persans, T.M. Hayes, Phys. Rev. B 52 (1995) 11763.
[38] Y. Kayanuma, Phys. Rev. B 38 (1988) 9797.
[39] N. Safta, A. Sakly, H. Mejri, Y. Bouazra, Eur. Phys. J. B 51 (2006) 75–78.
[40] A. Sakly, N. Safta, A. Mejri, H. Mejri, A. Ben Lamine, J. Nanomater (2010), ID746520.
[41] A. Sakly, N. Safta, H. Mejri, A. Ben Lamine, J. Alloys Compd. 476 (2009) 648–652.
[42] N. Safta, A. Sakly, H. Mejri, M.A. Zaïdi, Eur. Phys. J. B 53 (2006) 35–38.